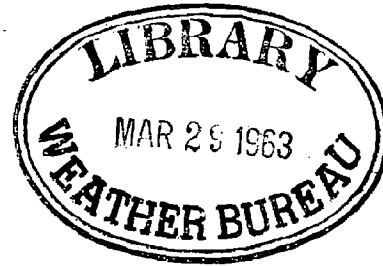


U.S. Numerical Weather Prediction
Group

UNITED STATES DEPARTMENT OF COMMERCE

WEATHER BUREAU

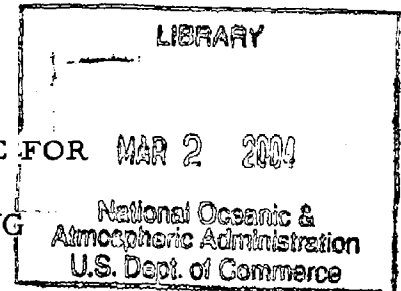


NATIONAL METEOROLOGICAL CENTER

TECHNICAL MEMORANDUM NO. 22

A THREE-LEVEL MODEL SUITABLE FOR MAR 2 2004

DAILY NUMERICAL FORECASTING



by

George P. Cressman
Director
National Meteorological Center

RAREBOOK

QC

996

T33

no. 22

Washington, D. C.

1963

122 722

National Oceanic and Atmospheric Administration

U.S. Joint Numerical Weather Prediction Unit

ERRATA NOTICE

One or more conditions of the original document may affect the quality of the image, such as:

Discolored pages
Faded or light ink
Binding intrudes into the text

This has been a co-operative project between the NOAA Central Library, National Center for Environmental Prediction and the U.S. Air Force. This project includes the imaging of the full text of each document. To view the original documents, please contact the NOAA Central Library in Silver Spring, MD at (301) 713-2607 x124 or www.reference@nodc.noaa.gov.

LASON
Imaging Contractor
12200 Kiln Court
Beltsville, MD 20704-1387
April 13, 2004

ABSTRACT

This paper describes a three-level numerical prediction model and its prediction capabilities. The calculation is made in two phases, diagnostic and prognostic. The diagnostic calculation consists of solving an equation for the vertical velocity, with the relation between the horizontal wind and the geopotential expressed by the balance equation. The field of vertical velocity is then used to obtain a velocity potential for use in the prognostic equation, where the wind consists of a nondivergent and an irrotational component. The calculation is carried out for the 800, 500, and 200 mb levels. Mountain effects and surface friction are included.

The performance of the model has been evaluated by comparison of the 500 mb forecasts of the three-level model with those of the barotropic. The three-level model forecasts motion and development on the planetary scale with some inaccuracies, but without any particular bias toward unrealistic retrogression. These inaccuracies are controlled artificially, in practice. On the smaller scale it is capable of forecasting non-barotropic development, depending on the strength of the actual and thermal jet streams and on their phase relative to each other. Waves in which the temperature field lags behind the pressure field amplify, and vice versa. The occlusion process is observed to take place in the forecasts. Comparative verifications of heights and winds show the three-level model to give significantly better forecasts than the barotropic.

Principal sources of residual error in the model are probably both vertical and horizontal truncation error as well as the neglect of nonadiabatic heat sources and sinks and the use of inexact forms of the equations of motion. However, the importance of various error sources can be correctly evaluated only after accomplishing their removal. Further work oriented toward this end is outlined.

A THREE-LEVEL MODEL SUITABLE FOR DAILY NUMERICAL FORECASTING

1. Introduction

Forecasts made by a model which is essentially barotropic have proved very useful over a period of several years, especially when augmented by a forecast of thickness in the layer from 850-500 mbs, enabling the prediction of vertical velocity and of flow patterns at different levels, e. g., at 850 mb directly, at 700 mb by interpolation, or at 300 or 200 mb by extrapolation. These forecasts, however, have limitations which have by now become well-known. The forecasts of 500 mb flow, as well as the vertically-measured flow, are inadequate in areas of strong temperature advection (baroclinic areas). Also, it is not possible to make satisfactorily accurate upward extrapolations from 500 mb to levels above the tropopause. Barotropic forecasts are also inadequate in areas dominated by the subtropical jet stream, which has as a rule a vertical profile of horizontal wind which is strongly peaked at high levels and is characteristically associated with a non-divergent surface well above 500 mb. [14]

Following the diagnostic study described in [7] it seemed desirable to construct a baroclinic forecasting model as an extension of the three-level diagnostic model described in the study. This model would then include, in addition to the normal barotropic effects, an estimate of mid-tropospheric divergence and its effects, the effects of vertical advection of momentum,

and a more accurate estimate of mountain effects and surface friction than can be obtained by a single-parameter model. Additionally, there would be a higher level than 500 mb carried explicitly throughout the forecast, eliminating the difficulties inherent in upward extrapolation from lower levels.

Numerous forecasts made previously at many places using the geostrophic wind approximation in a multi-level forecast model have shown several serious limitations of this type of wind approximation as actually applied. The geostrophic divergence has large-scale destructive effects, [12] excessive cyclogenesis takes place, indicating a too rapid rate of energy conversion in the forecasts, and the required linearization of the divergence term in the vorticity equation leads to excessive intensity of anticyclones, especially if the forecasts are carried out to 48 hours or more on a hemispheric grid [4].

In order to avoid these difficulties as far as possible a representation of the wind field was used for this model in which the wind is obtained as a second approximation, given as a sum of a non-divergent component and an irrotational component. The non-divergent component is used as a first approximation to obtain a divergence, which is then used to obtain the irrotational component. The resulting wind approximation then permits the use of a more exact form of the vorticity equation, which is used as the prognostic equation. This is an essential feature of the model. A detailed discussion of this problem can be found in the paper by Lorenz [8]. The reader will

discover that the system of equations described below resembles in many respects the system proposed by Lorenz, in which he uses the balance equation as a filtering approximation and develops an energy-conserving set of model equations.

A serious limitation on the accuracy obtainable by the model is imposed by the use of only three levels in the vertical. The neglect of details of the low-level temperature field and the truncation errors involved in representing the vertical profile of wind, especially near the tropopause [7], seem to be serious deficiencies, and an increase of the number of levels from three to four or five appears very desirable. A four level model is now in preparation in an effort to reduce some of these deficiencies. However, the results obtained from forecasting with the three-level model have indicated its basic usefulness, and daily forecasting with it has begun. This paper is therefore written as an interim measure for limited distribution to describe the presently used model without waiting for completion and testing of the four-level version, which will require some time.

2. The Atmospheric Model

The atmospheric state and motion are represented by information at three basic levels, i. e., 800, 500, and 200 mb. This information consists of the geopotentials at these levels and the derived parameters. These are represented in Figure 1, and are:

- (a) The stream function ψ at each level, obtained from the balance equation,

$$\nabla^2 \psi = \frac{1}{f} \left\{ \nabla^2 \Phi + 2 \left[\left(\frac{\partial^2 \psi}{\partial x \partial y} \right)^2 - \frac{\partial^2 \psi}{\partial x^2} \frac{\partial^2 \psi}{\partial y^2} \right] - \nabla \psi \cdot \nabla f \right\} \quad (2.1)$$

where Φ is geopotential, f is the Coriolis parameter, and ψ is the stream function.

(b) The velocity potential χ at each level, obtained from equation (2.8).

(c) The wind at each level, obtained from (a) and (b) above, as described by equation (2.4) and (2.7).

(d) The stream function at the standard pressure of the surface of the ground, obtained by interpolation or downward extrapolation from 500 and 800 mb.

(e) The vertical velocity at the ground, obtained from equation (2.9).

Since 800 mb is not a standard reporting surface, 800 mb data are obtained by interpolation between 500 and 850 mbs.

The calculation is made in two separate steps -- diagnostic and prognostic. The diagnostic vertical-velocity equation is obtained from the well-known vorticity and energy equations

$$\frac{\partial \zeta}{\partial t} + \underline{V} \cdot \nabla \eta - \eta \frac{\partial \omega}{\partial p} + k \cdot \nabla \times \omega \frac{\partial \underline{V}}{\partial p} = 0 \quad (2.2)$$

$$\frac{\partial}{\partial t} \left(\frac{\partial \Phi}{\partial p} \right) + \underline{V} \cdot \nabla \frac{\partial \Phi}{\partial p} + \omega \sigma = 0 \quad (2.3)$$

In equations (2.2) and (2.3) \underline{V} is the horizontal wind; ζ is the relative vorticity; η is the absolute vorticity; $\omega = dp/dt$, the vertical velocity in

the pressure coordinate system; \underline{k} is a unit vector in the vertical; and σ is a measure of the static stability given by $\sigma = -\alpha \partial \ln \theta / \partial p$, where α is specific volume and θ is potential temperature.

For the purpose of obtaining the diagnostic equation, we will make certain simplifications which will not all be carried over into the prognostic equations. For the purpose of calculating horizontal advection we will assume that the horizontal wind is non-divergent, and can be represented by a stream function, i. e.,

$$\underline{V} = \underline{k} \times \nabla \psi. \quad (2.4)$$

We will further assume that the static stability varies only in the vertical. Finally, in order to obtain an equation for ω it is necessary to eliminate the local time derivatives by specifying some relation between wind and temperature. For this limited purpose, we introduce the geostrophic approximation in the form

$$\frac{\partial}{\partial t} \left(\frac{\partial \Phi}{\partial p} \right) = f \frac{\partial}{\partial t} \left(\frac{\partial \psi}{\partial p} \right). \quad (2.5)$$

An interesting possibility would be the use of the balance equation for this relationship, but this was not done.

Introduction of the above approximations into equation (2.2) and (2.3) leads to the ω - equation:

$$\nabla^2 \omega + \frac{\eta f}{\sigma} \frac{\partial^2 \omega}{\partial p^2} + \frac{f}{\sigma} \frac{\partial \eta}{\partial p} \frac{\partial \omega}{\partial p} - \frac{f}{\sigma} \frac{\partial}{\partial p} (\underline{k} \cdot \nabla \times \omega \frac{\partial V}{\partial p}) = \frac{1}{\sigma} \left[f \frac{\partial}{\partial p} (\underline{V} \cdot \nabla \eta) - \nabla^2 (\underline{V} \cdot \nabla \frac{\partial \Phi}{\partial p}) \right] \quad (2.6)$$

The fourth term on the left side of the equation, while not difficult to include in the computations, increases the time required for solution for ω , and adds to the data handling problems in the computer. Several tests consisting of solving equation (2.6) with and without this term indicated no significant contributions of the term to the resulting fields of ω . In the interests of economy this term was therefore dropped from the calculations, and will not appear in further discussion of the diagnostic equation.

The approximation of setting $\frac{\partial \sigma}{\partial x} = \frac{\partial \sigma}{\partial y} = 0$, mentioned earlier, may be a serious one, and was examined at length. This consisted of allowing σ to vary freely, thus increasing the model from an essentially three-parameter model to a five-parameter one. This addition increased both the computing time and the data handling problem significantly, without contributing to any interesting reduction of errors in the forecast flow patterns. While the test was made on only a small number of meteorological situations, the tentative conclusion was reached that the results did not justify the extra work, and no further efforts in this direction were made.

Another test was made in which the advecting wind in the ω - equation was permitted to be divergent, i. e. ,

$$\underline{V} = \underline{k} \times \nabla \psi + \nabla \chi, \quad (2.7)$$

χ being the velocity potential. This was accomplished by an iterative procedure, χ being obtained from values of ω from each preceding scan by the

use of the continuity equation in the form

$$\nabla^2 \chi + \partial \omega / \partial p = 0 \quad (2.8)$$

No difficulty was experienced in obtaining convergence to a final value of ω . However, the difference obtained in the resulting forecasts made from the diagnostic quantities was quite insignificant, not justifying the additional computer time required.

The upper and lower boundary conditions required for ω are $\omega = 0$ at $p = 0$ and $\omega = \omega_g$ at $p = 1000$ mbs. One variant tried was to set $\omega = \omega_g$ at $p = p_g$, the pressure at the ground. No difficulties were encountered, but the differences introduced were small and not very interesting, and the earlier version, being simpler, is now used. The values of ω_g are obtained from including the effects of the air rising and sinking over a smoothed set of mountains, and from the effects of surface friction. The details of the mountain and friction effects are the same as those used in the barotropic model described in [6] with the exceptions that the surface wind components, u_g and v_g are obtained from a stream function extrapolated downward to p_g from the 800 and 500 mb stream functions carried internally. The lower boundary condition is therefore given by the equation

$$\omega_g = \bar{v}_g \cdot \nabla p_g + \frac{g}{f} \left[\frac{\partial}{\partial y} (C_d u_g \sqrt{u_g^2 + v_g^2}) - \frac{\partial}{\partial x} (C_d v_g \sqrt{u_g^2 + v_g^2}) \right] \quad (2.9)$$

where g is the gravitational acceleration, and C_d is the drag coefficient given by

$$C_d = \frac{\tau}{\rho |V_g|^2} \quad (2.10)$$

Here, ρ is the surface density, V_g is understood as the wind at the top of the friction layer, but is referred to in this discussion as the surface wind, and τ is the surface stress. The values of p_g developed by Berkofsky and Bertoni [2] and the values of C_d published in map form by Cressman in [6] were used.

The diagnostic calculation is completed by calculating the velocity potential, χ , at each level from equation (2.8). This is necessary for calculation of the divergent wind for use in the prognostic equation, which is the vorticity equation (2.2) put in the following form with the aid of equations (2.7) and (2.8).

$$\frac{\partial}{\partial t} (\nabla^2 \psi) + J(\psi, \eta) + \nabla \cdot \eta \nabla^2 \chi + \nabla \cdot \omega \nabla \frac{\partial \psi}{\partial p} = 0 \quad (2.11)$$

where J is the Jacobian operator. This form of the equation is obtained by neglecting the divergent part of the wind in the fourth term in equation (2.2). Thus, with the appropriate boundary conditions

$$\int_A \frac{\partial}{\partial t} (\nabla^2 \psi) dA = 0$$

The importance of obtaining an exactly zero integral of $\frac{\partial}{\partial t} (\nabla^2 \psi)$ over the forecast area has been stressed by Wiin Nielsen [15] and by Arnason and Carstensen [1]. If this is not done, very destructive systematic errors will quickly ruin the forecast.

The calculation of the new stream functions for the next time step is completed by a centered extrapolation from the previous time step except for the first time step, when a forward extrapolation is used. The use of a one-hour time step is sufficient to avoid computational instability except at 200 mb, where half-hour time steps are used. This is done without the necessity for a new solution of the ω - equation at the half-hour interval by making the assumption that all the ω terms in equation (2.2), the prognostic equation, are constant for the full hour period. Following the solution for the new 200 mb stream function at the half-hour interval a new value of $J(\psi, n)$ is computed and equation (2.2) can then be solved again for $\partial\zeta/\partial t$ and $\partial\psi/\partial t$, which is then used to obtain the new value of the 200 mb stream function at the end of the second half-hour period.

The completion of the calculation of the new values of stream functions allows the calculation of the new geopotentials at each level by the inversion of the balance equation, equation (2.1).

The order of calculations is schematically described by the flow chart shown in Figure 2.

3. The Finite Difference System and Constants

The application of finite differences to the balance equation will not be discussed here, since this is a separate and difficult subject. The method of solution used at the National Meteorological Center was developed here by

Shuman. His method of solution is described in [13] and the finite difference scheme now used is basically similar to the one described by Miyakoda [9] as "Method B (9-point system)."

Essentially, two grid-increment horizontal differences were used throughout for representation of horizontal derivatives centered on the intermediate point. The finite-difference Laplacian and Jacobian operators applying at point 13 in Figure 3 can be written as

$$\nabla_a^2 = a_{23} + a_{11} + a_3 + a_{15} - 4a_{13}, \text{ and} \quad (3.1)$$

$$J(a, b) = (a_{14} - a_{12})(b_{18} - b_8) - (a_{18} - a_8)(b_{14} - b_{12}) \quad (3.2)$$

In some forecasts, a four grid-increment wave appeared by 24 hours, with an approximately constant rate of amplification, resulting in some undesirable aspects of the prognostic charts by that time. This difficulty was greatly suppressed by replacing (3.2) by a 9-point Jacobian due to L. Carstensen and given for point 13 with reference to Figure 3 as

$$\begin{aligned} J(a, b) = & 1/2 [(a_{13} - a_{17})(b_{18} - b_{12}) - (a_{18} - a_{12})(b_{13} - b_{17})] \quad (3.3) \\ & + 1/2 [(a_{14} - a_{18})(b_{19} - b_{13}) - (a_{19} - a_{13})(b_{14} - b_{18})] \\ & + 1/2 [(a_8 - a_{12})(b_{13} - b_7) - (a_{13} - a_7)(b_8 - b_{12})] \\ & + 1/2 [(a_9 - a_{13})(b_{14} - b_8) - (a_{14} - a_8)(b_9 - b_{13})] \end{aligned}$$

The use of coefficients of 1/2 before each term instead of values of 1/4 represent the adjustment of the final value to the basic 2 grid-increment distance used throughout the rest of the program. Despite the formidable appearance of this operator, it can be programmed to run on the computer in only a trivially longer time than the operator of equation (3.2).

The ω equation in finite difference form is written for each of the two levels involved, the two equations being solved simultaneously, namely:

$$\nabla^2 \omega_{3/2} - A_1 \omega_{3/2} = F_1 + A_2 \omega_{5/2} \quad (3.4)$$

$$\nabla^2 \omega_{5/2} - A_3 \omega_{5/2} = F_2 + A_4 \omega_{3/2} + A_5 \omega_g \quad (3.5)$$

where

$$A_1 = \left(\frac{1}{5.25 \times 10^{10}} \right) \frac{d^2}{m^2} \left(\frac{\eta f}{\sigma} \right)_{3/2} \quad (3.6)$$

$$A_2 = \left(\frac{1}{9.75 \times 10^{10}} \right) \frac{d^2}{m^2} \left(\frac{f}{\sigma} \right)_{3/2} \eta_2 \quad (3.7)$$

$$A_3 = \left(\frac{1}{5.25 \times 10^{10}} \right) \frac{d^2}{m^2} \left(\frac{\eta f}{\sigma} \right)_{5/2} \quad (3.8)$$

$$A_4 = - \left(\frac{1}{9.75 \times 10^{10}} \right) \frac{d^2}{m^2} \left(\frac{f}{\sigma} \right)_{5/2} \eta_2 \quad (3.9)$$

$$A_5 = - \left(\frac{1}{9.75 \times 10^{10}} \right) \frac{d^2}{m^2} \left(\frac{f}{\sigma} \right)_{5/2} \eta_3 \quad (3.10)$$

$$F_1 = \frac{1}{3 \times 10^5 \sigma_{3/2}} \{ f[\mathcal{J}(\psi_2, \eta_2) - \mathcal{J}(\psi_1, \eta_1)] - \nabla^2 \frac{m^2}{2d^2} [\mathcal{J}(\psi_1 + \psi_2)(\Phi_2 - \Phi_1)] \}, \quad (3.11)$$

and

$$F_2 = \frac{1}{3 \times 10^5 \sigma_{5/2}} \left\{ f \left[\mathcal{J}(\psi_3, \eta_3) - \mathcal{J}(\psi_2, \eta_2) \right] - \nabla^2 \frac{m^2}{2d^2} \left[\mathcal{J}(\psi_2 + \psi_3)(\bar{\Phi}_3 - \bar{\Phi}_2) \right] \right\} \quad (3.12)$$

The subscripts in equations (3.4) through (3.12) refer to the vertical indices (see Figure 1), d is the mesh length, and m is the map scale factor. The term $(f/\sigma) (\partial\eta/\partial p) (\partial\omega/\partial p)$ appearing in equation (2.6) is absorbed in equations (3.4) and (3.5) to a very good approximation by the appropriate choice of absolute vorticity on the right-hand side of equations (3.7) and (3.9) when the finite differences in the vertical are formed.

The values of the mean static stability were taken from values given by Peixoto [10], and represent the average atmospheric static stabilities typical of the south edge of the principle jet stream, where the most active baroclinic systems appear, giving values of 5.0×10^{-4} and 2.2×10^{-4} in c. g. s. units for $\sigma_{3/2}$ and $\sigma_{5/2}$, respectively.

The horizontal mesh length, d is taken as 762 km, i. e., two grid lengths.

The prognostic equation become

$$\nabla^2 \frac{\partial \psi_1}{\partial t} = -\mathcal{J}(\psi_1, \eta_1) - \nabla \cdot \eta_1 \nabla \chi_1 - \frac{4}{7\Delta p} (\nabla \cdot \omega \nabla \psi')_{3/2} \quad (3.13)$$

$$\nabla^2 \frac{\partial \psi_2}{\partial t} = -\mathcal{J}(\psi_2, \eta_2) - \nabla \cdot \eta_2 \nabla \chi_2 - \frac{3}{10\Delta p} [(\nabla \cdot \omega \nabla \psi')_{3/2} + (\nabla \cdot \omega \nabla \psi')_{5/2}] \quad (3.14)$$

and

$$\nabla^2 \frac{\partial \psi_3}{\partial t} = -\mathcal{J}(\psi_3, \eta_3) - \nabla \cdot \eta_3 \nabla \chi_3 - \frac{4}{7\Delta p} (\nabla \cdot \omega \nabla \psi')_{5/2} \quad (3.15)$$

where

$$(\nabla \cdot \omega \nabla \psi')_k = \nabla \cdot \omega_k \nabla (\psi_k + 1/2 - \psi_k - 1/2) \quad (3.16)$$

and

$$\Delta p = 3 \times 10^5$$

The term $\nabla \cdot \eta \nabla \chi$ is evaluated by the following expression (referring to Figure 3) as

$$\nabla \cdot \eta \nabla \chi = (\chi_{15} - \chi_{13}) \bar{\eta}_{14} - (\chi_{13} - \chi_{11}) \bar{\eta}_{12} + (\chi_{23} - \chi_{13}) \bar{\eta}_{18} - (\chi_{13} - \chi_3) \bar{\eta}_8, \quad (3.17)$$

where

$$\bar{\eta}_{14} = 1/4 (\eta_{13} + 2\eta_{14} + \eta_{15}), \text{ etc.} \quad (3.18)$$

4. Solution on the Computer

This model is currently running on the NMC IBM 7090, using full 32,768 word memory and 5 tapes for program and erasable storage, with an additional tape for the history of the calculation and another tape for output data. Running time is almost exactly two minutes per hour of forecast, including about fifty seconds for inversion of the balance equation for the three levels each hour of the forecast. The length of time required for the output processing depends on the number of maps required as well as the type of processing required, such as printing, preparation for the curve

follower, or punching. The elements for which maps can be made available are those represented in Figure 1 or their derivatives.

5. Performance Characteristics

The model described above was tested on a wide variety of atmospheric situations. The performance characteristics shown by these tests can be discussed with reference to the scale of the system described. It is most convenient to describe the treatment of the planetary scale systems first, since certain difficulties encountered here resulted in a slight change to the model.

The non-divergent barotropic model, as is well known by now, gives forecasts characterized by a fictitious retrogression of the planetary scale waves. This is controlled in practice by the addition to the model of a divergence given by

$$\nabla \cdot \underline{V} = - \frac{\mu}{\bar{\psi}} \frac{\partial \psi}{\partial t} \quad (5.1)$$

where $\bar{\psi}$ is a mean value of the 500 mb stream function and μ is assigned a value of 8 or 4 (see Bolin [3] and Cressman [5]). The behaviour of the barotropic forecasts is not very sensitive to variations of μ in this range.

A. Wiin-Nielsen [16] in an analysis of a three parameter model resembling in many respects the one described in this paper examined the 500 mb divergence in very long waves. He found that it has a distribution which counteracts the tendency for retrogression of these systems and found the divergence on the largest horizontal scale to depend critically on the

curvature of the vertical profile of wind. It was therefore a matter of considerable interest to see whether or not the three-level model described here would forecast the planetary wave patterns correctly.

The behaviour of the model in this respect can be summarized by saying that it made forecasts of the planetary scale components to move or develop in different directions, according to the particular situation being examined. There did not appear to be any tendency for systematic erroneous retrogression in the forecasts, as was the case with the non-divergent barotropic model. Forecasts of eastward movement of wave numbers one or two were not uncommon. However, in certain special situations, the movement and development of the planetary wave components appeared to be overforecast (forecast of too much change). In view of Wiin-Nielsen's analysis, it would seem that truncation error in a three-level representation of the vertical profile of wind could account for inaccurate forecasts of planetary scale systems. It should be emphasized that this problem did not assume serious proportions except on very rare occasions. However, a model used for daily forecasting must be protected, so far as is possible, from errors which become serious only on rare occasions.

Although the desirability from a scientific point of view for any empirical type of remedy for this problem is debatable, the urgency of the situation in daily forecasting is compelling, and a protection against large errors of this type was adopted. This remedy, which consisted of the introduction of an

artificial divergence proportional to the local stream function tendency into the prognostic equation, was found to work quite satisfactorily. This is similar to the barotropic divergence initially proposed by Rossby [11] and analyzed in detail by Yeh [17]. The prognostic equation (2.11) was therefore modified to include such a divergence, becoming

$$\left(\nabla^2 - \frac{\mu\eta}{\psi}\right) \frac{\partial\psi}{\partial t} + \mathcal{J}(\psi, \eta) + \nabla \cdot \eta \nabla \chi + \nabla \cdot \omega \nabla \frac{\partial\psi}{\partial p} = 0 \quad (5.2)$$

Equations (3.13), (3.14), and (3.15) then become

$$\left(\nabla^2 - \frac{\eta_1}{m^2\psi_1}\right) \frac{\partial\psi_1}{\partial t} = -\mathcal{J}(\psi_1, \eta_1) - \nabla \cdot \eta_1 \nabla \chi_1 - \frac{4}{7\Delta p} (\nabla \cdot \omega \nabla \psi')_{3/2}, \quad (5.3)$$

(5.4)

$$\left(\nabla^2 - \frac{\eta_2}{m^2\psi_2}\right) \frac{\partial\psi_2}{\partial t} = -\mathcal{J}(\psi_2, \eta_2) - \nabla \cdot \eta_2 \nabla \chi_2 - \frac{3}{10\Delta p} [(\nabla \cdot \omega \nabla \psi')_{3/2} + (\nabla \cdot \omega \nabla \psi')_{5/2}],$$

and

$$\left(\nabla^2 - \frac{\eta_3}{m^2\psi_3}\right) \frac{\partial\psi_3}{\partial t} = -\mathcal{J}(\psi_3, \eta_3) - \nabla \cdot \eta_3 \nabla \chi_3 - \frac{4}{7\Delta p} (\nabla \cdot \omega \nabla \psi')_{5/2}. \quad (5.5)$$

The magnitudes of the coefficients were determined empirically. At 500 mb (level 2) the magnitude of the coefficient μ in equation (5.2) is unity, one-fourth the value used here in operational barotropic forecasting. It is therefore seen that the additional divergence is very small, affording a slight

but advantageous dampening on the forecast movements of the planetary scale systems.

If our interpretation of the problem by means of Wiin-Nielsen's analysis is correct, one could anticipate even less trouble with planetary scale components of the flow if four levels of data instead of three were carried. Work now in progress will, in due time, throw more light on this problem.

On a somewhat shorter scale, the performance of the three-level model is similar to that of the barotropic much of the time, with important differences that depend on the relative phases of the horizontal pressure and temperature waves. If the temperature wave lags behind the pressure wave, amplification of the pressure wave occurs. The rate of dampening and amplification depends on the intensity of the wind and thermal jet streams as well as on the horizontal scale of the systems. Relatively large scale systems, other things being equal, amplify the most rapidly; and a minimum scale for amplification exists in this model. It is certain that a similar lower scale limit does not exist in the atmosphere.

An example of a pronounced out-of-phase wave is observed in the situation of February 15, 1962. The disturbance in the Greenland area amplified into one of the worst storms to hit N. W. Europe in many years. The sequence of 850 mb charts shown in Figures 4, 5, and 6, demonstrate the process of occlusion, in which the size of the warm sector is diminished

at the same time as the phase lag of the temperature wave decreases, with the cold air catching up with the low level cyclone. Figures 7, 8, 9, and 10, show the 500 mb forecasts from the three-level and barotropic models. Here we can see that the barotropic forecasts contained some of the mechanism for the storm formation, but that the contribution of the baroclinic process was very important. The verifications are shown in Figures 11 and 12.

In examining the performance of the model in the smallest part of the spectrum resolvable in the grid, we find that there is a distinct tendency for very small scale systems to move too slowly in the forecast. This is probably attributable to truncation error, especially in the finite-difference Jacobian.

6. Verification

A period suitable for comparative verifications extends from 13 April to 16 June 1962. During this time the three-level model was run in its present form, without any changes. At the same time barotropic forecasts were made from the same data. A total of 44 forecasts from each model from the same data can then be compared. This has been done for five separate areas as well as for the whole grid. The results are shown in Table 1. The key to the different areas is shown in Figure 13. The interpretation of these verifications is complicated by the fact that the barotropic forecast model had a feedback into the verifying analyses through the first guess for each analysis, giving the barotropic forecast an unfair advantage. This is not serious for the good data areas, but is more likely to bias the results for the poor data

areas, where the first guess has a greater influence on the final analysis. The least bias is probably found for the North American (I) and European (III) areas - just those areas showing the greatest improvement over the barotropic forecasts. The consistency of the improvement obtained from the three-level forecasts is shown in Figures 14 and 15. To obtain these the 44 three-level forecasts were arranged in chronological order and separated into eight groups of five each, with four in the last group. These are indicated by the period number along the abscissa of each graph. The r. m. s. height errors of each forecast (three-level), barotropic, and persistence, are represented as a function of the period. The consistently better performance of the three-level model is evident from these graphs. The decreasing error level observed from left to right on the diagrams is a result of the decreasing strength of the circulation as the season advances. There is also a probable decrease in over-all baroclinic activity as the warmer season comes (see Figure 15).

7. Special Problems

The analysis of the initial data is a more critical problem for baroclinic than for barotropic forecasting, since if the correct baroclinic processes are to be represented by the model, the vertical structure at the initial time must be correctly analyzed. This can become a severe problem in large areas not containing observations.

An example of this type of difficulty occurred during the middle of March 1962, when the repetitive processes in the objective analysis program

led to a representation of a low latitude jet stream along the lower left slant boundary of the grid, west and southwest of Mexico. This jet stream was represented as having a strong increase of strength from 850 to 500 mbs, but little vertical shear from 500 to 200 mb. No data at all were reported from this region. This led to 500 mb divergence patterns having far-reaching and destructive consequences. The magnitude of these was assessed by re-analyzing the initial data and eliminating the low latitude jet stream, which never had been supported by any data, and then making a new forecast from the reanalyzed data. The differences in the new and the original 36-hour forecasts were a maximum in the southeast United States, and would have been very significant for weather forecasting. Since the low-latitude jet stream had a rather large extent, there were significant differences on a large scale between the two 36-hour forecasts, with differences of 200 feet as far away as Greenland.

The problem of obtaining at least a harmless analysis in the several low-latitude areas of no data should be partly solved by a recent change in the objective analysis system. However, other analysis problems exist which have not been solved and which may prove troublesome. It will be necessary to get more experience with these before any remedies can be attempted.

8. Conclusions and Further Plans

It is not possible to document completely in a paper of this type all the significant characteristics of a new forecast model by showing examples of the forecasts. As a substitute for an extensive set of figures, the following characteristics can be enumerated:

- a. The three-level model is much better at forecasting planetary scale waves than a non-divergent barotropic model, but still needs some help in the form of an artificial divergence, which is, however, much smaller than that required in barotropic forecasting.
- b. Baroclinic developments occurring on a fairly large scale are successfully forecast by the three-level model. Many smaller scale developments ($L < \text{about } 1200 \text{ km}$), which sometimes appear with considerable intensity at the low levels, are inadequately forecast. It has not yet been determined whether this is a consequence of a lack of sufficient vertical or horizontal resolution, the lack of consideration of latent heat of condensation, or something else.
- c. The three-level model is much more successful than the barotropic at forecasting the displacement and development of the lower latitude systems associated with the subtropical jet stream.
- d. The three-level model provides more accurate mountain and surface friction effects on the forecasts than does the barotropic, due to the better surface wind available for calculating these effects. This is particularly useful in forecasting displacement of cut-off lows in the S. W. United States.

In planning future developments, one naturally concentrates on the inadequacies of the present systems, with the hope of removing them. A four-level model is now in an advanced stage of checkout. With this, it

should be possible to obtain a reduced truncation error in using vertical derivatives of the wind. According to Wiin-Nielsen, this ought to result in an improvement in obtaining the divergence in mid-troposphere, especially for the planetary-scale systems. It should also give a somewhat better picture of the lower-level temperature field than the three-level model does. At the same time, experiments are being continued on a new finite-difference operators with the hope of reducing horizontal truncation error. Also, sufficient storage is provided in the computer code for the four-level model to permit the introduction of the effects of surface heating and possibly the latent heat of condensation.

The limiting factor on accuracy of this type of model is not definitely known, but may be the introduction of the geostrophic approximation for the tendencies in equation (2.5). The restriction imposed on static stability is not essential in the framework of this model, but if removed will substantially increase the computing time, probably to the extent where a primitive equation model would be less expensive to compute. In any event, the relative performance of the primitive and filtered equation models must be evaluated, since neither approach to the solution of the basic equations seems to have been more than partially exploited.

TABLE 1

ROOT-MEAN-SQUARE ERRORS OF 36 HR 500 MB FORECASTS

APRIL 13 - JUNE 16

Area	Persistence		Barotropic		3-Level	
	Wind Error (knots)	Height Error (feet)	Wind Error (knots)	Height Error (feet)	Wind Error (knots)	Height Error (feet)
I	21	225	14	165	13	149
II	25	277	16	179	15	168
III	24	274	15	163	14	153
IV	21	221	14	163	14	168
V	25	272	16	176	15	170
Grid	20	213	14	154	13	148

CAPTIONS

- Fig. 1 Parameters used at different levels.
- Fig. 2 Flow chart indicating the order of calculations.
- Fig. 3 Grid points used in finite-difference operators.
- Fig. 4 850 mb chart for 00GMT, 15 February 1962. Solid lines are
 850 mb contours. Dashed lines show 850-500 mb thickness.
- Fig. 5 24 hour 850 mb and 500-850 mb forecast from 00GMT,
 15 February 1962.
- Fig. 6 48 hour 850 mb and 500-850 mb forecast from 00GMT,
 15 February 1962.
- Fig. 7 500 mb, 00GMT, 15 February 1962.
- Fig. 8 24 hour 500 mb forecast from 00GMT, 15 February 1962 (3-level
 model).
- Fig. 9 48 hour 500 mb forecast from 00GMT, 15 February 1962 (3-level
 model).
- Fig. 10 48 hour barotropic 500 mb forecast from 00GMT, 15 February 1962.
- Fig. 11 850 mb and thickness 500-850 mb, 00GMT, 17 February 1962.
- Fig. 12 500 mb, 00GMT, 17 February 1962.
- Fig. 13 Verification areas.
- Fig. 14 R. M. S. height error of 36-hr 500 mb forecasts -- Area I.
- Fig. 15 R. M. S. height error of 36-hr 500 mb forecasts -- entire grid
 area.

9. REFERENCES

1. G. Arnason and L. Carstensen, "The Effects of Vertical Vorticity Advection and the Turning of Vortex Tubes in Hemispheric Forecasts with a Two-Level Model," Monthly Weather Review, Vol. 87, No. 4, April 1959, pp. 119-127.
2. L. Berkofsky and E. A. Bertoni, "Mean Topographic Charts for the Entire Earth," Bulletin of the American Meteorological Society, Vol. 36, No. 7, Sept. 1955, pp. 350-354.
3. B. Bolin, "An Improved Barotropic Model and Some Aspects of Using the Balance Equation for Three-Dimensional Flow," Tellus, Vol. 8, No. 1, Feb. 1956, pp. 61-75.
4. J. G. Charney, B. Gilchrist, and F. G. Shuman, "The Prediction of General Quasi-Geostrophic Motions," Journal of Meteorology, Vol. 13, No. 5, Oct. 1956, pp. 489-499.
5. G. P. Cressman, "Barotropic Divergence and Very Long Atmospheric Waves," Monthly Weather Review, Vol. 86, No. 8, Aug. 1958, pp. 293-297.
6. G. P. Cressman, "Improved Terrain Effects in Barotropic Forecasts," Monthly Weather Review, Vol. 88, Nos. 9-12, Sept-Dec 1960, pp. 327-342.
7. G. P. Cressman, "A Diagnostic Study of Mid-Tropospheric Development," Monthly Weather Review, Vol. 89, No. 3, Mar. 1961, pp. 74-82.

8. E. N. Lorenz, "Energy and Numerical Weather Prediction," Tellus,
Vol. 22, No. 4, Nov. 1960, pp. 364-375.
9. K. Miyakoda, "Numerical Solution of the Balance Equation," Technical
Report J. M. A., No. 3, Aug. 1960, pp. 15-34.
10. J. P. Peixoto, "Hemispheric Conditions During the Year 1950," Planetary
Circulation Project, Mass. Inst. of Tech., Scientific Report
No. 4, Nov. 1960, 211 pp.
11. C. G. Rossby and Collaborators, "Relation Between Variations in the
Intensity of the Zonal Circulation of the Atmosphere and the
Displacements of the Semi-Permanent Center of Action,"
Journal of Marine Research, Vol. 2, No. 1, 1939, pp. 38-55.
12. F. G. Shuman, "Predictive Consequences of Certain Physical Inconsistencies
in the Geostrophic Barotropic Model," Monthly Weather Review,
Vol. 85, No. 7, July 1957, pp. 229-234.
13. F. G. Shuman, "Numerical Methods in Weather Prediction: I. The
Balance Equation," Monthly Weather Review, Vol. 85, No. 10,
Oct. 1957, pp. 329-332.
14. H. Taba, "The Horizontal and Vertical Wind Profile of the Subtropical
and Polar Jet for January 1-7, 1956 and the Variation of the
Equivalent Barotropic Level," Tellus, Vol. 11, No. 4, Nov.
1959, pp. 441-451.
15. A. Wiin-Nielsen, "On Certain Integral Constraints for the Time-Integration
of Baroclinic Models," Tellus, Vol. 11, No. 1, Feb. 1959,
pp. 45-59.

16. A Wiin-Nielsen, "Diagnosis of Divergence in a Three-Parameter Numerical Prediction Model," Monthly Weather Review, Vol. 89, No. 3, Mar. 1961, pp. 67-73.
17. T. C. Yeh, "On Energy Dispersion in the Atmosphere," Journal of Meteorology, Vol. 6, No. 1, Feb. 1949, pp. 1-16.

Vertical Index	Pressure
$k = 1$ ——— ψ, ϕ, χ ———	200 Mb
$3/2$ — — ω — — — —	350
2 ——— ψ, ϕ, χ ———	500
$5/2$ — — ω — — — —	650
3 ——— ω, ϕ, χ ———	800
$-(\psi, \phi)$ — — — —	850



Fig. 1 Parameters used at different Levels

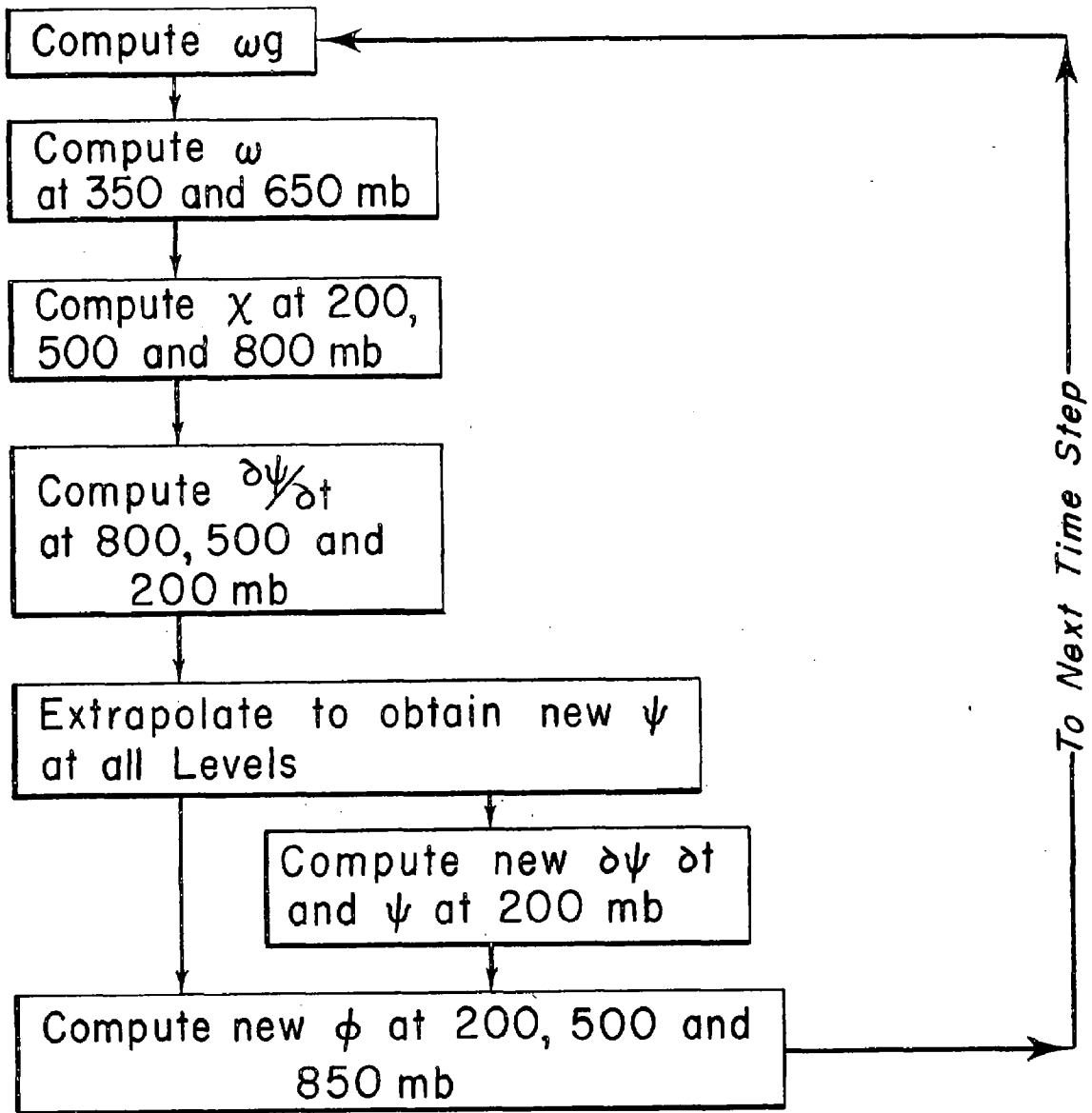


Fig. 2 Flow Chart indicating the Order of Calculations

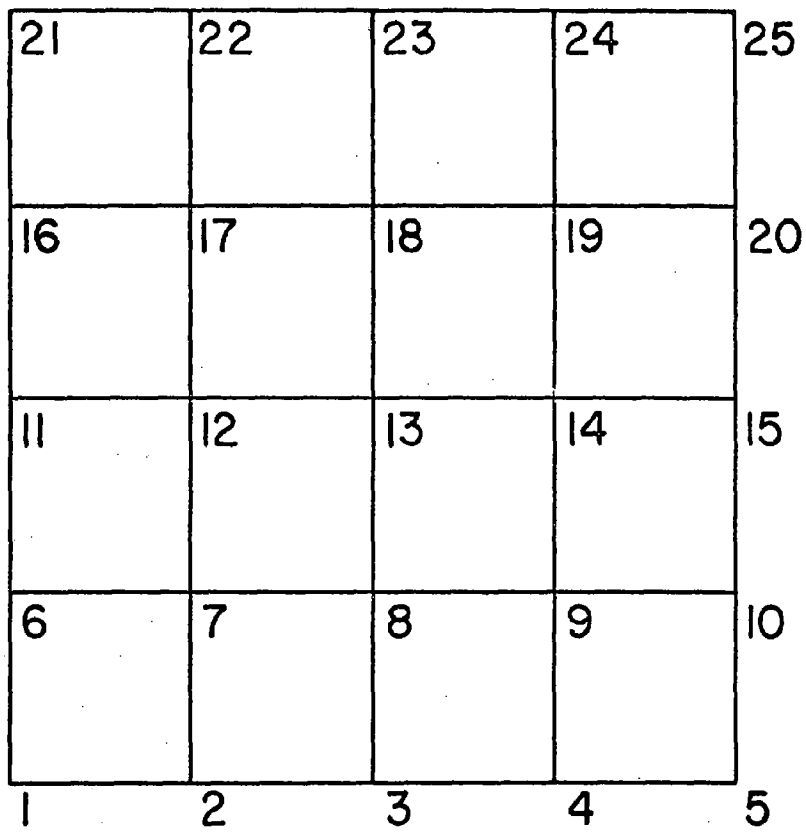
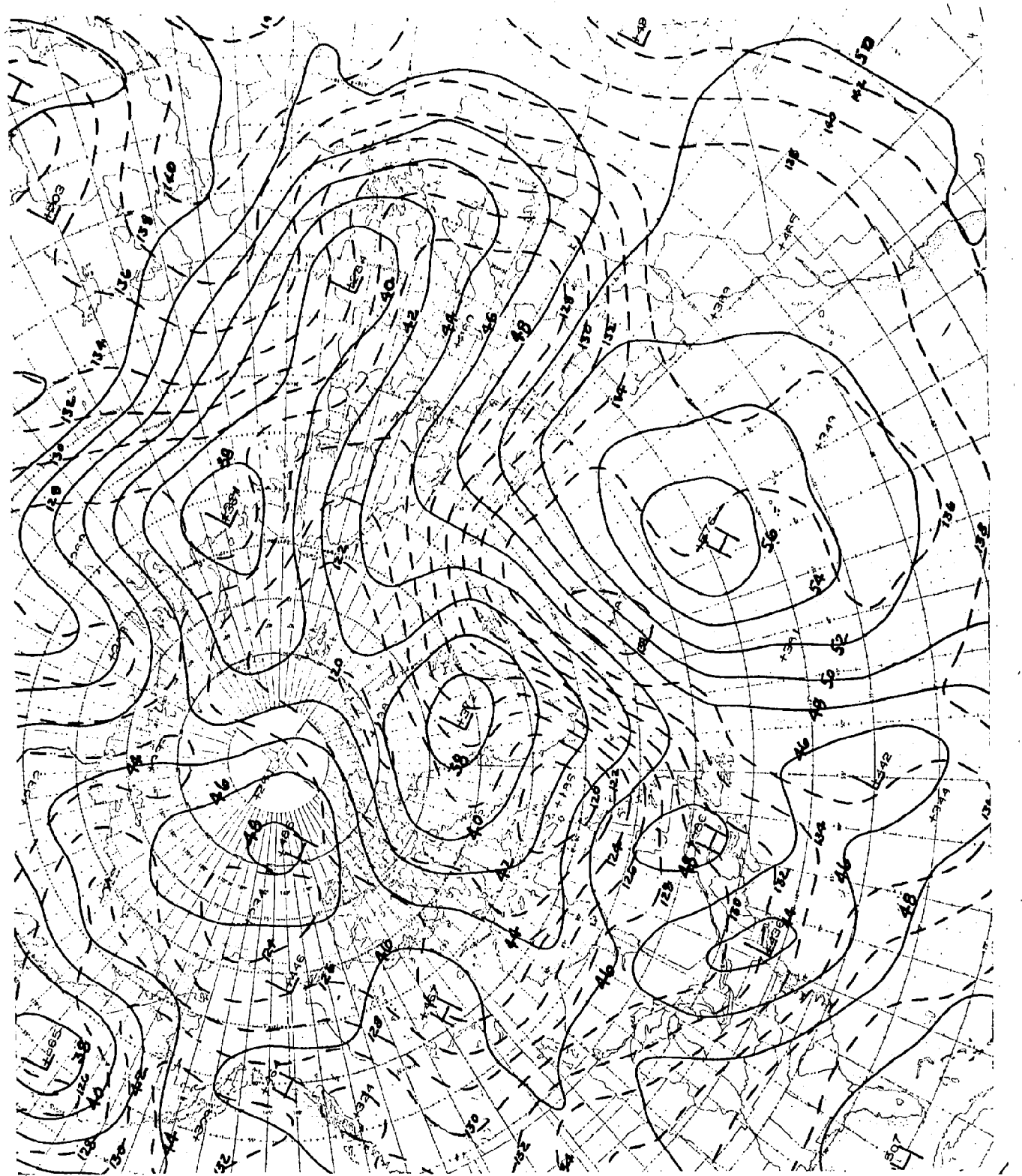
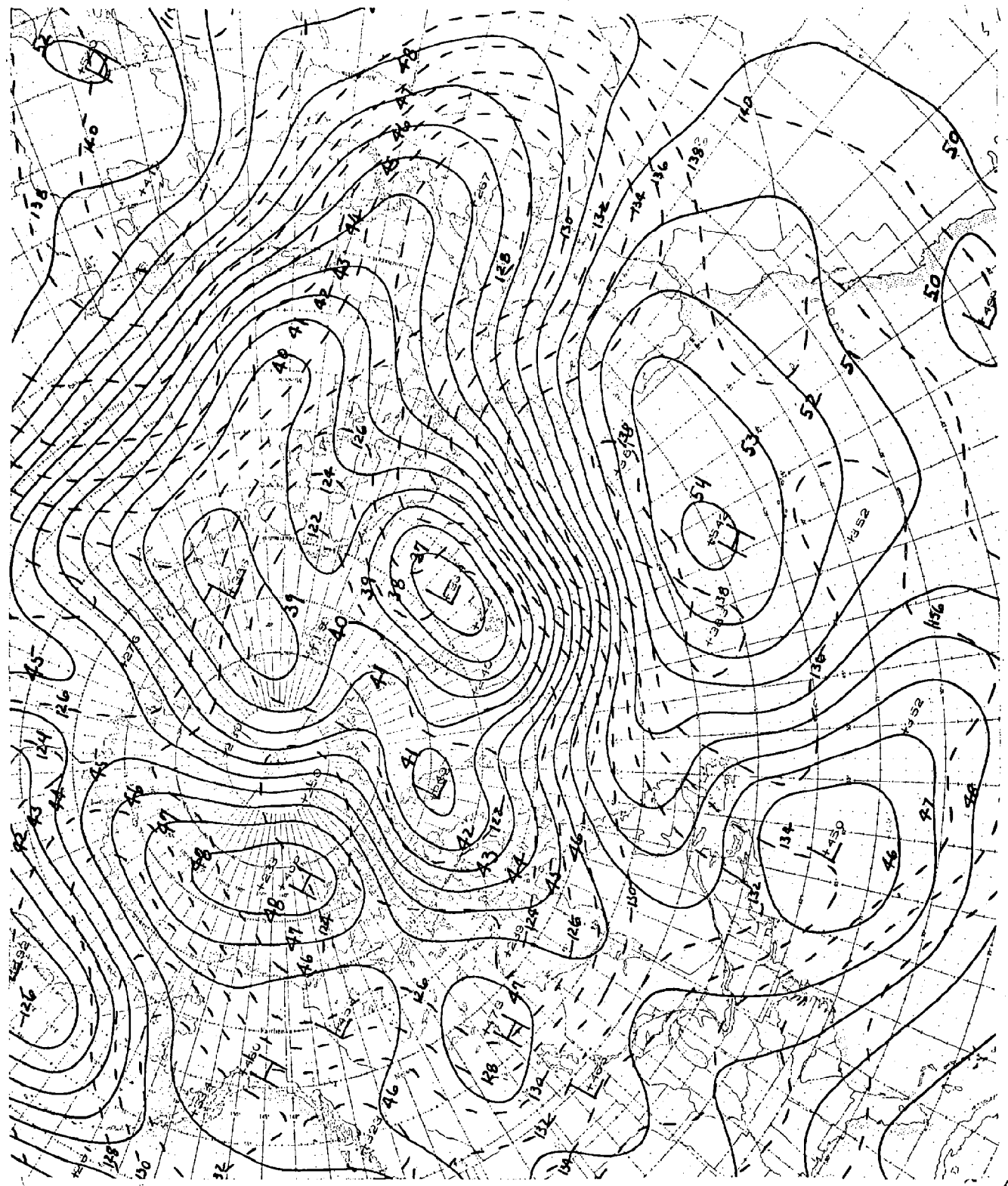
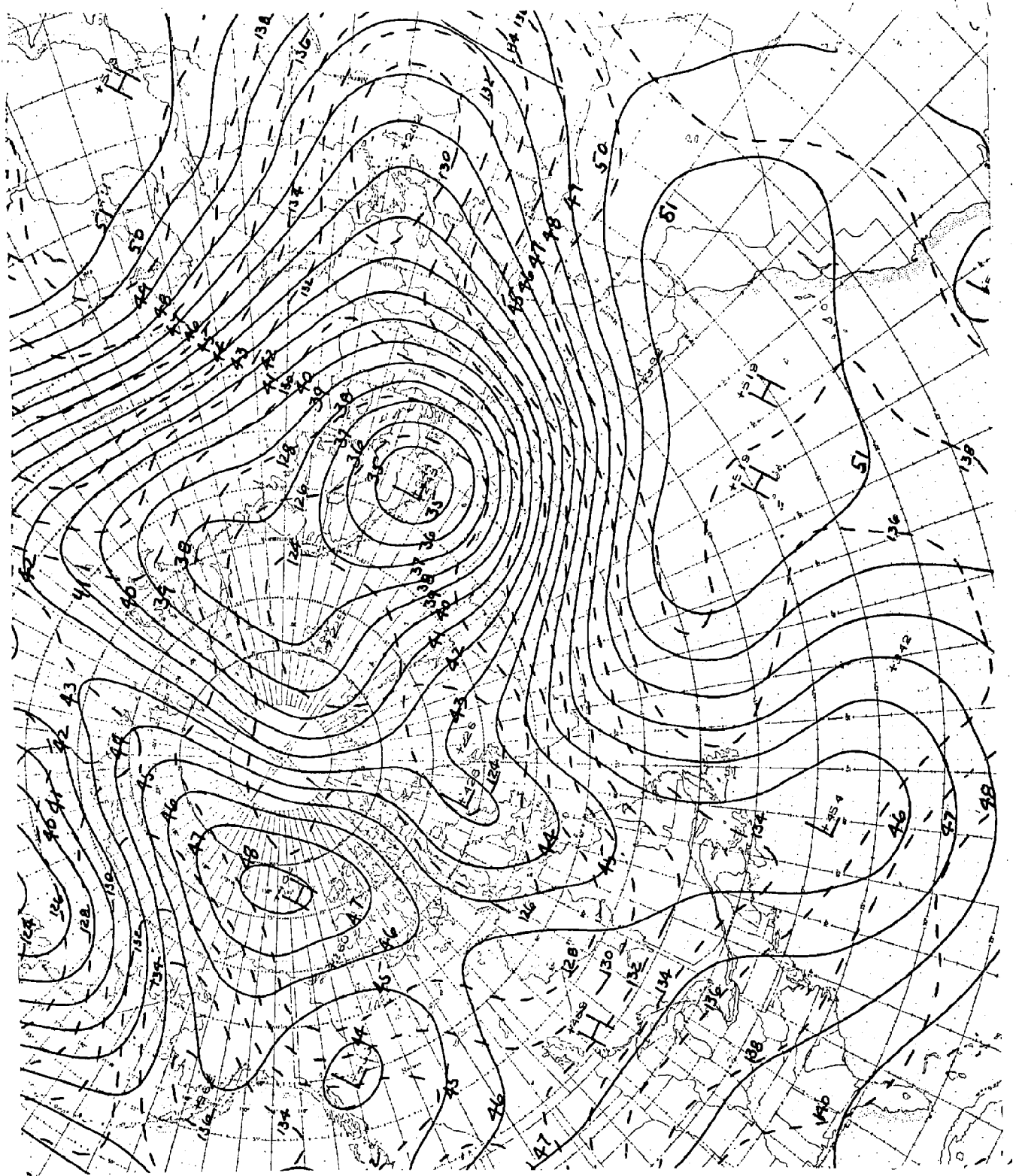
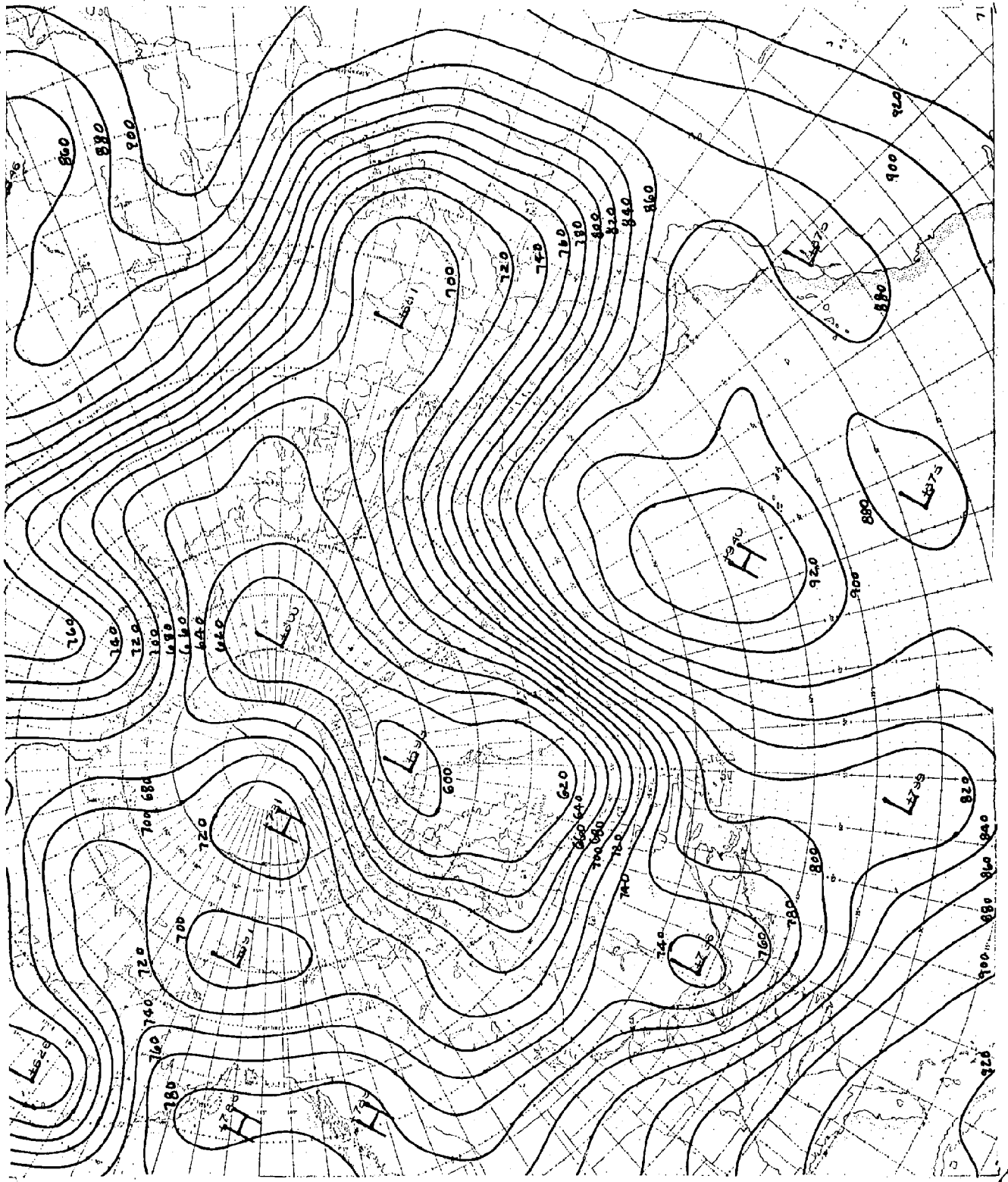


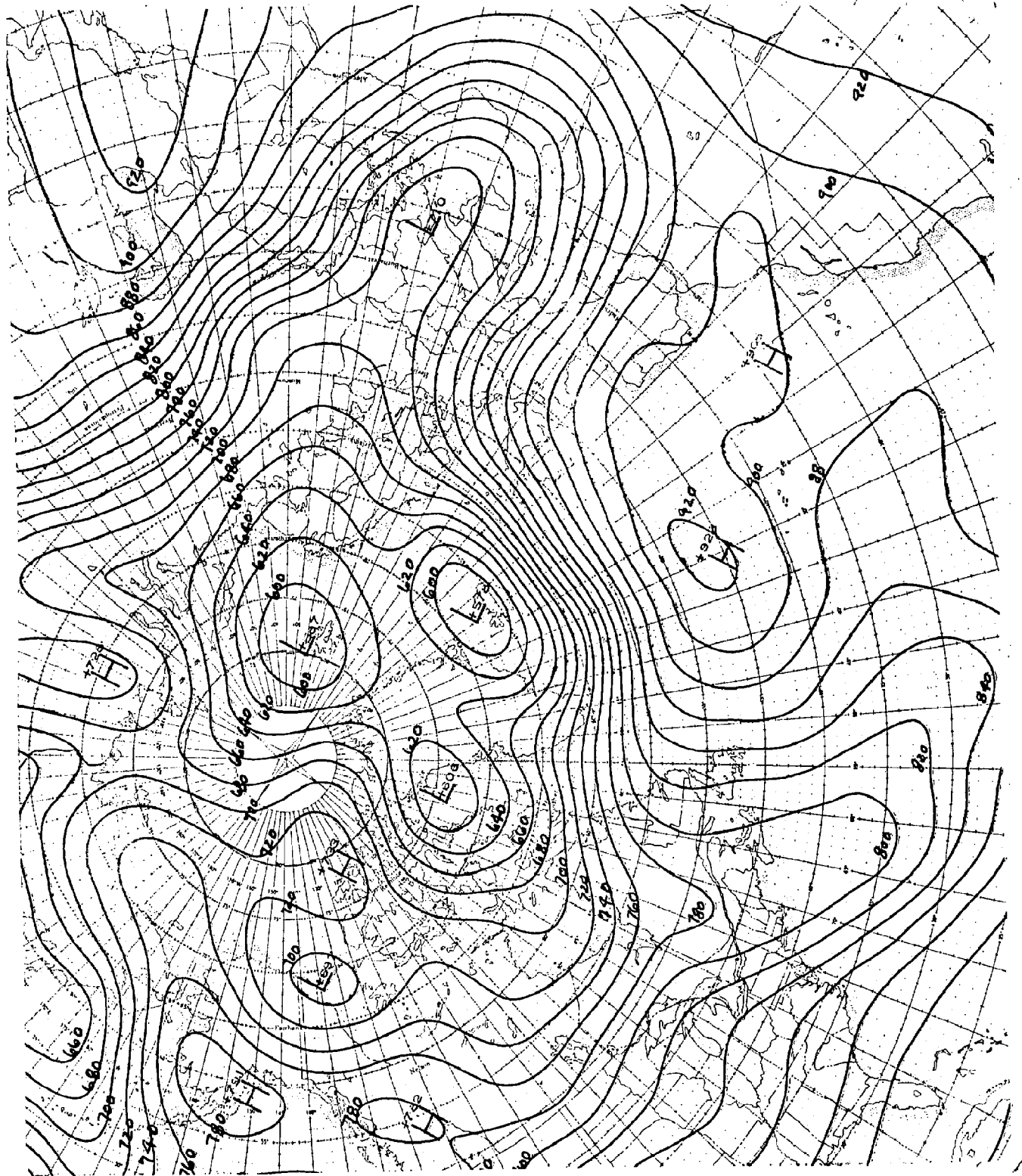
Fig. 3 Grid Points used in Finite-difference Operators

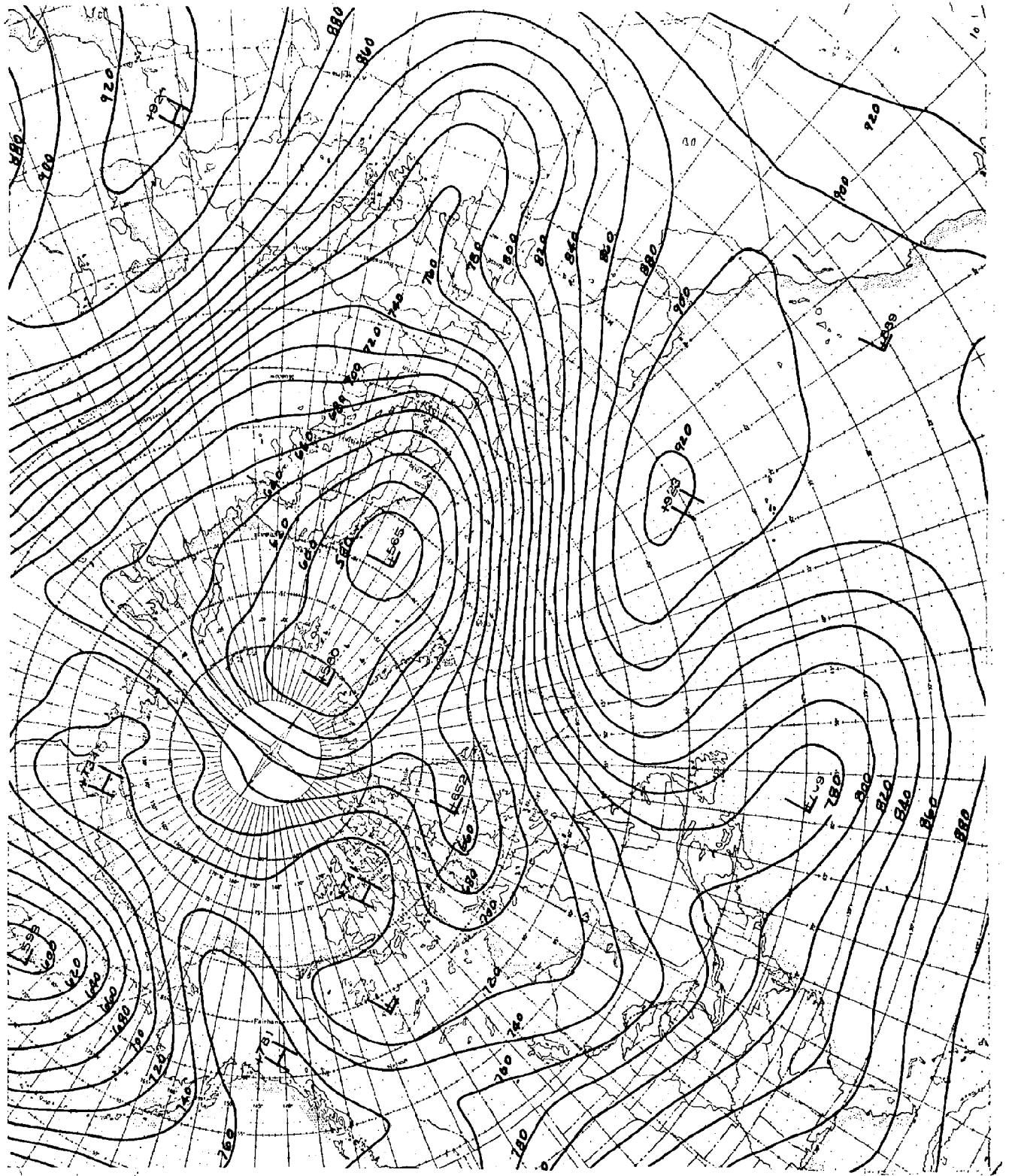


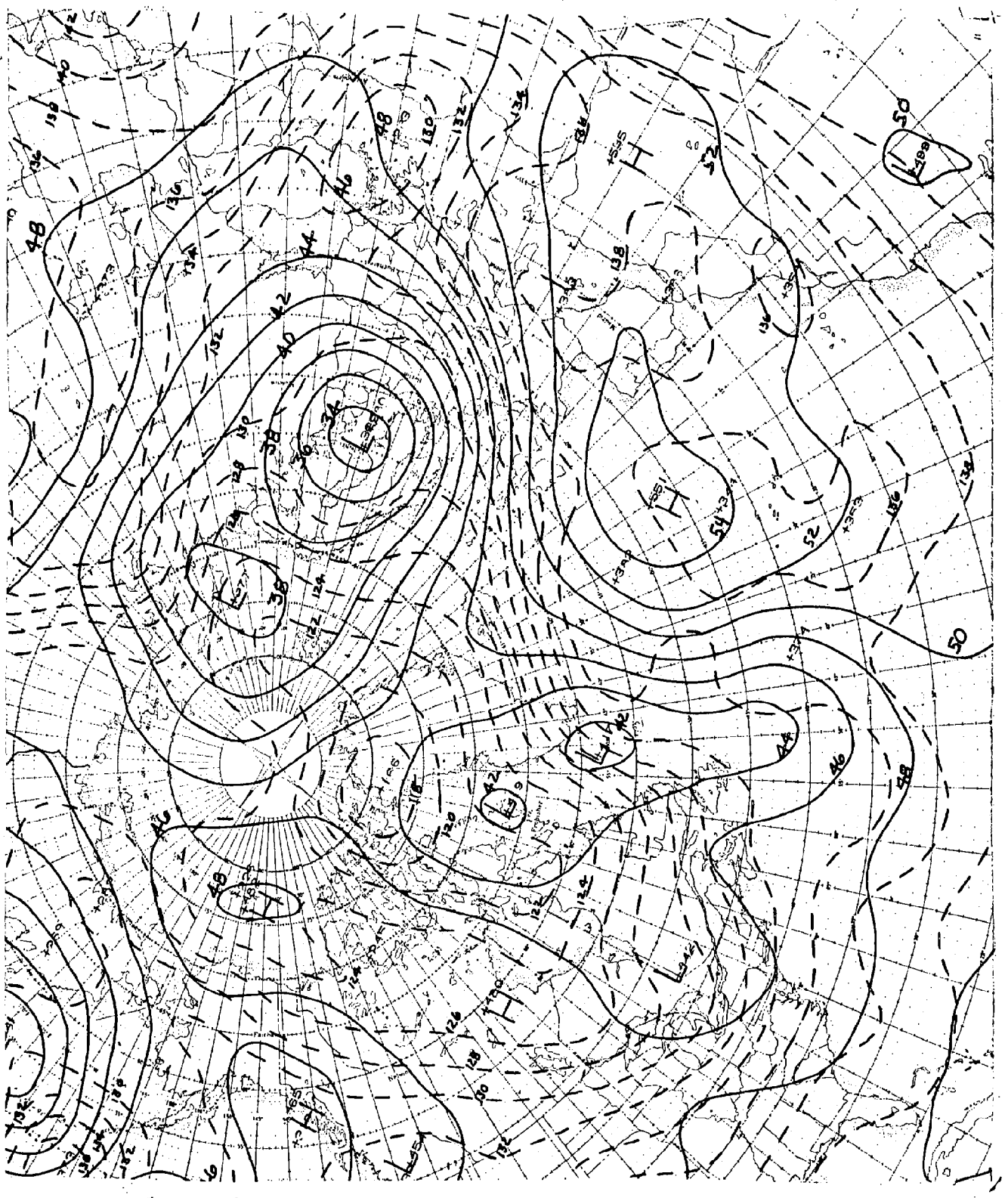


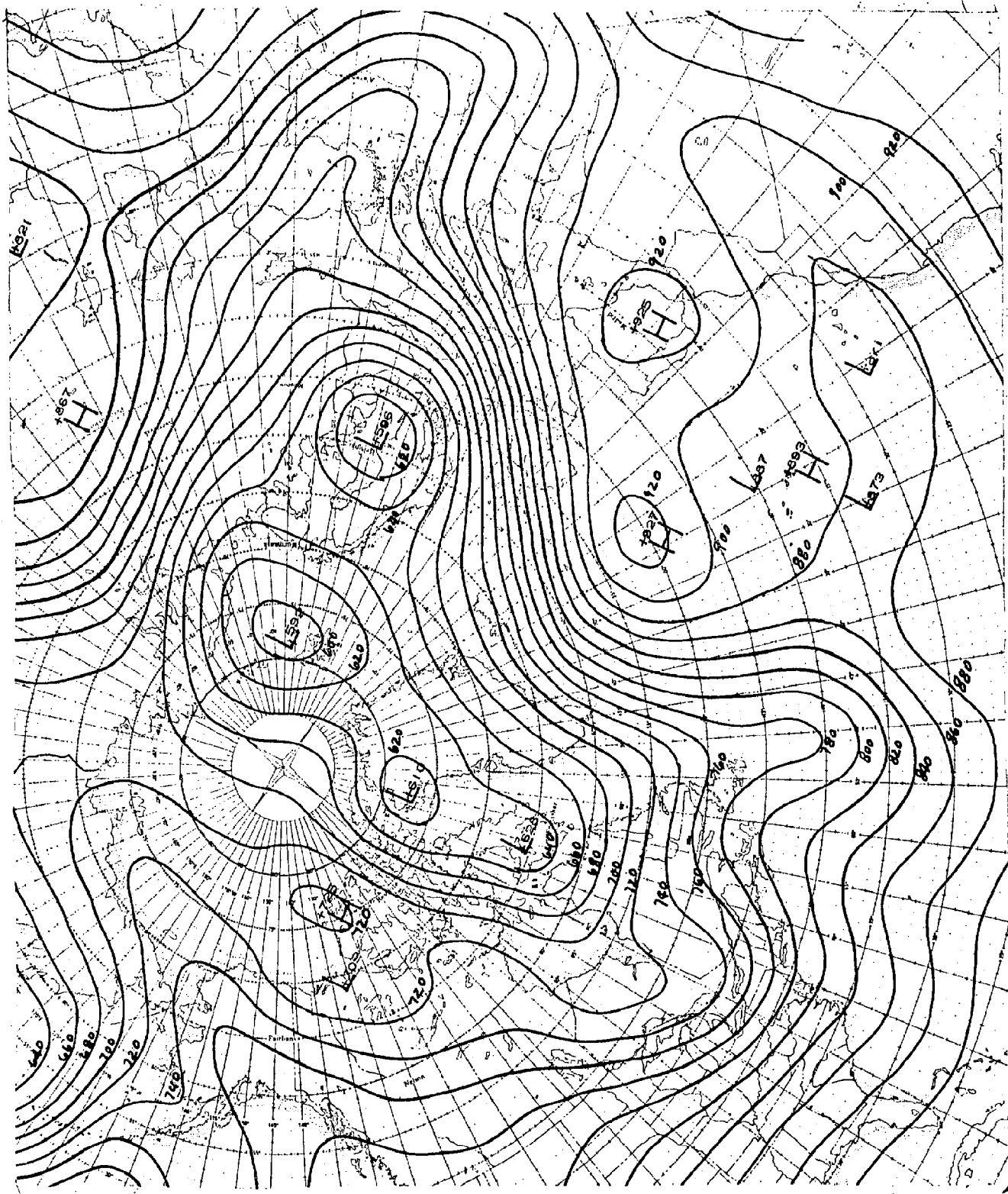












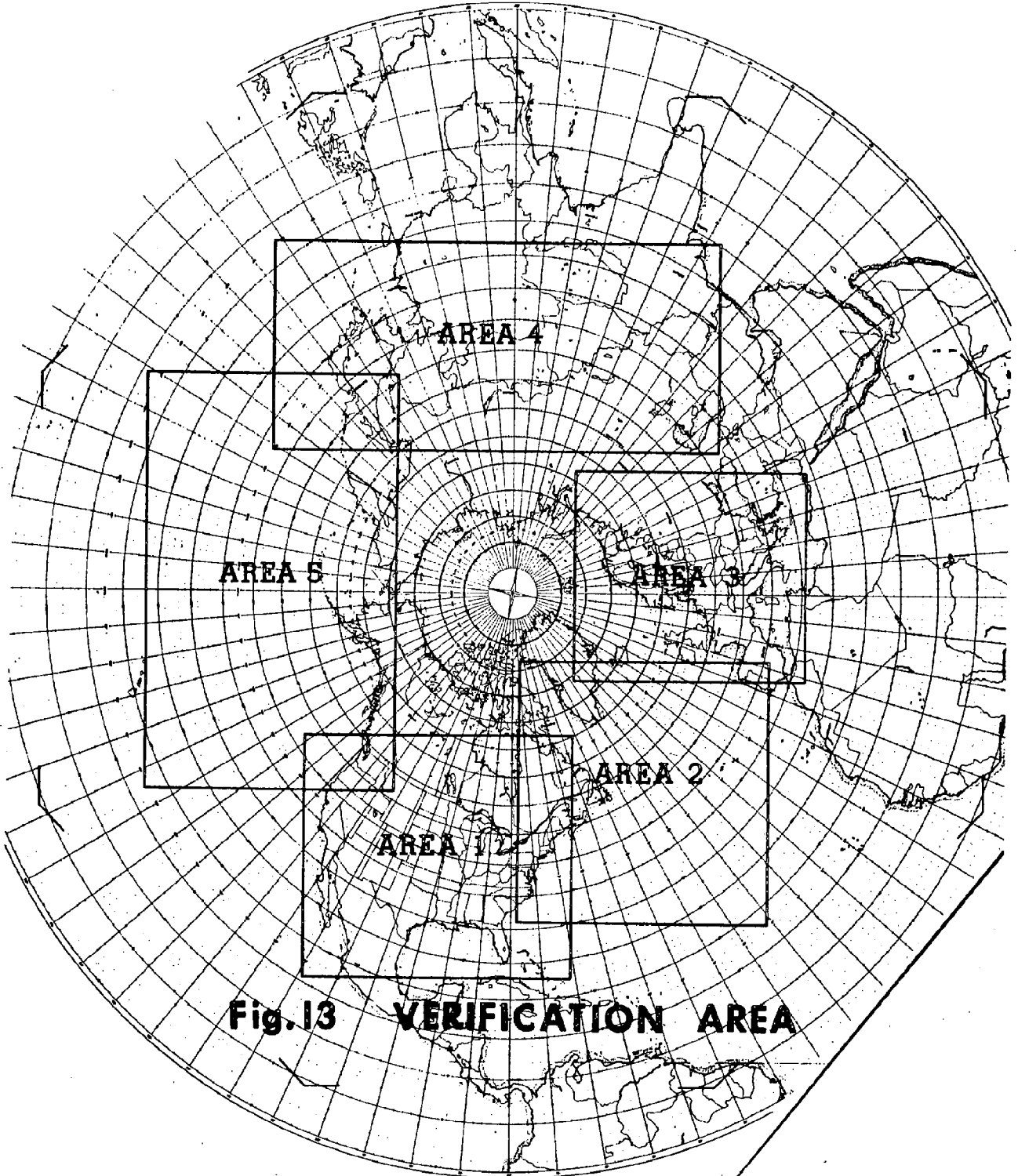


Fig. 13 VERIFICATION AREA

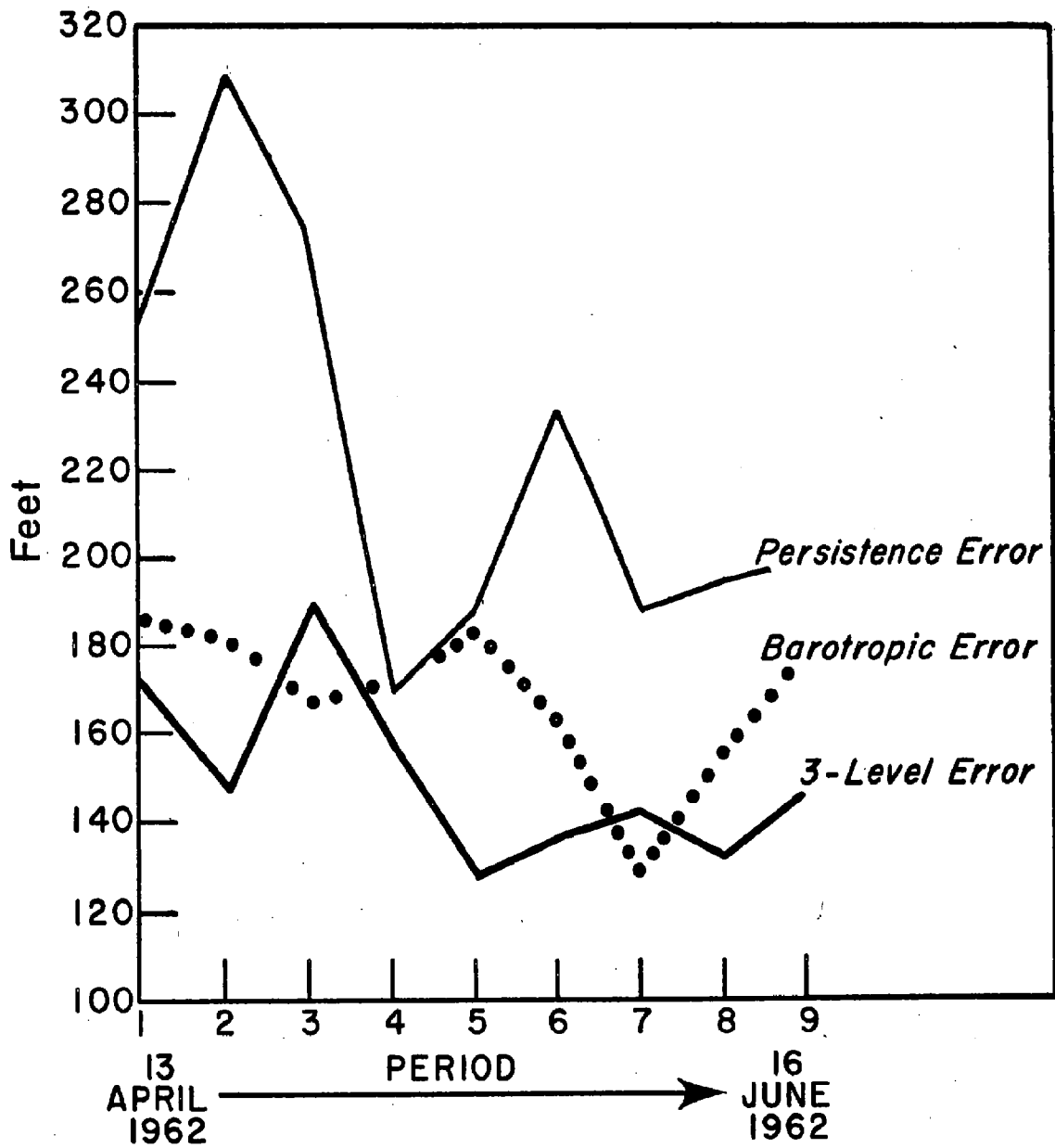


Fig. 14 R.M.S. Height Error of 36-hour 500 mb Forecasts— Area 1

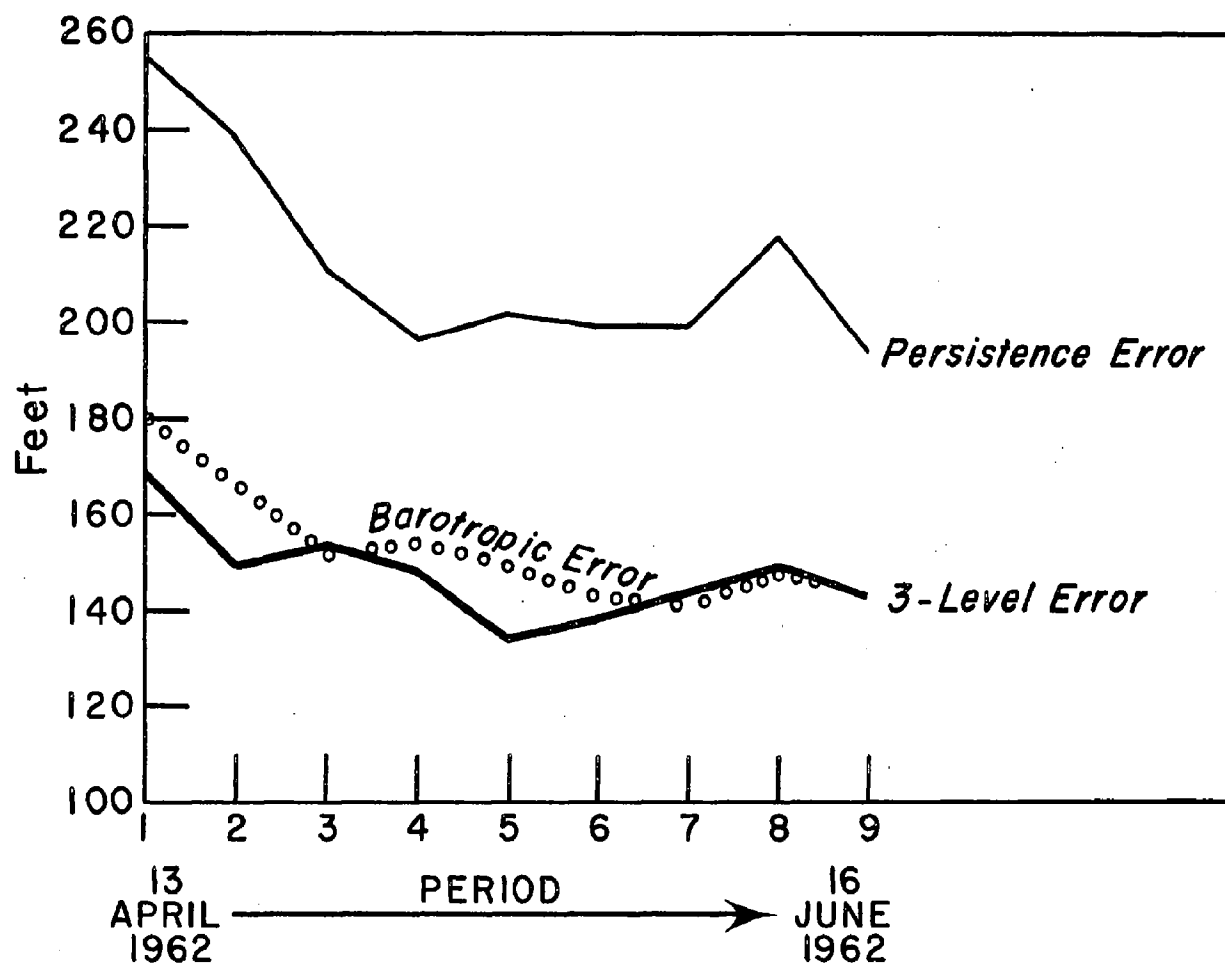


Fig. 15 R.M.S. Height Error of 36-hour 500 mb Forecasts Entire Grid Area